ELSEVIER

Thermochimica Acta 360 (2000) 109–120

thermochimica acta

www.elsevier.com/locate/tca

Mechanism of carbothermal reduction of iron, cobalt, nickel and copper oxides

Boris V. L'vov*

Department of Analytical Chemistry, St. Petersburg State Technical University, St. Petersburg 195251, Russia

Received 5 January 2000; received in revised form 4 April 2000; accepted 8 April 2000

Abstract

A new scheme of thermal dissociation which is based on the dissociative evaporation of the reactant with simultaneous condensation of the low-volatile product has been invoked to interpret the kinetics of reduction of FeO, CoO, NiO and Cu_2O by carbon. A critical analysis of literature data and their comparison with theoretical calculations has shown that the main kinetic characteristics of carbothermal reduction, including the initial decomposition temperature and activation energy are in full agreement with the proposed mechanism of decomposition. Condensation of the low-volatile product (metal vapour) in the reaction zone and partial transport of condensation energy to the oxide account for the features which are typical of solid state reactions and manifest themselves in the appearance of periods of induction and acceleration in the course of the process. Carbon fulfils the role of buffer in this process. This is supported by an appearance of metals in the condensed phase and a higher than equilibrium partial pressure of oxygen in high-vacuum experiments with Knudsen cells.

Keywords: Activation energy; Autocatalysis; Carbothermal reduction; Dissociative evaporation; Iron oxide; Initial temperature; Kinetics

1. Introduction

Carbothermal reduction of iron oxides is the oldest technological process, which defined the history of humans during the last 4000–5000 years starting from the beginning of the Iron Age [1]. Interest in the study of solid direct reduction of iron oxides is supported nowadays with its increased industrial application for the production of sponge iron [2].

No wonder that the mechanism of this reaction (and similar processes of carbothermal reduction of Co, Ni and Cu oxides) was a subject of numerous studies during this century. Several mechanisms have been proposed to explain the interaction of two solid reactants (oxide and carbon) at temperatures below 800–1000°C with the formation of solid metal. The oldest and most widespread is the mechanism of oxide reduction through gaseous intermediates CO and CO_2 in accordance with the following reactions:

$$MO(s) + CO \rightarrow M(s) + CO_2 \quad (1)$$

$$CO_2 + C(s) \rightarrow 2CO \quad (2)$$

Already in 1875, Gruner [3] discussed this mechanism in his classical book on metallurgy. In this century, Baikov [4], Pavlov [5], Chufarov [6] and Esin and Gel'd [7] in Russia were the active proponents of this mechanism. However, its application meets with some obstacles. The most important is a rather slow (and thermodynamically limited) restoration of CO at low temperatures. The other problems are connected with the interpretation of an autocatalytic effect observed

* Tel.: +7-812-552-7741; fax: +7-812-247-4384.
E-mail address: blvov@robotek.ru (B.V. L'vov).

0040-6031/00/$ – see front matter
PII: S0040-6031(00)00540-2

for all these oxides and the high rate of their reduction in vacuum. In connection with this, some alternative mechanisms have been proposed.

In the beginning of the 1980s, L'vov [8] proposed a mechanism of oxide reduction through gaseous carbides formed via the interaction of metal vapour with carbon

$$2MO(s) + MC_2(g) \rightarrow 3M(g) + 2CO \quad (3)$$

$$2C(s) + M(g) \rightarrow MC_2(g) \quad (4)$$

This mechanism has been supported by the direct observation of metal and gaseous carbide vapours by mass spectrometry. It was used for the interpretation of temporal oscillations in the kinetics of interaction of carbon with the oxides of different elements [9–11]. However, contrary to our preliminary expectations [9], this mechanism cannot be applied to the reduction of Fe, Co, Ni and Cu oxides owing to the low saturated pressure of metals at reduction temperatures and the impossibility of transportation of metal vapour to carbon in line with reaction (4).

Digonskii [12] recently proposed a mechanism of reduction through gaseous intermediates H_2 and H_2O:

$$MO(s) + H_2 \rightarrow M(s) + H_2O \quad (5)$$

$$C(s) + H_2O \rightarrow H_2 + CO \quad (6)$$

Hydrogen in the reaction mixture originates, in the author's opinion, from the water vapour adsorbed on the carbon surface. However, some doubts are cast upon the presence of H_2 in quantities which are necessary for the efficient reduction, especially in vacuum.

Baikov [4], Tammann and Sworykin [13] and Baikov and Tumarev [14] tried to use a thermal dissociation scheme for the interpretation of carbothermal reduction mechanism in accordance with the combination of reactions

$$MO(s) \rightarrow M(s) + \tfrac{1}{2}O_2 \quad (7)$$

$$C(s) + O_2 \rightarrow CO_2 \quad (8)$$

However, the equilibrium partial pressure of O_2 for reaction (7) is too small to explain real rates of reduction. For FeO and Cu_2O at 1200 K, $P(O_2)$ is 2×10^{-17} and 1×10^{-8} atm, respectively. For this reason, this scheme is usually denied by the majority of workers. The only exception are the studies by Kurchatov in the 1950s [15]. He observed, in particular, the presence of 8–9% O_2, 90–91% CO_2 and only 1% CO in the gaseous products generated in the process of heating of Cu_2O and graphite (in two different boats) in vacuum. This composition correlates well with the products for reactions (7) and (8) and disagrees with those for reactions (1) and (2). Besides, Kurchatov [15] has found that at 600–900°C, the partial pressure of O_2 over Cu_2O alone is comparable with that for the gaseous products (CO_2 and O_2) over Cu_2O and graphite located in different boats: 12 and 16 Torr at 600°C; 19 and 20 Torr at 700°C; 29 and 24 Torr at 800°C and 32 and 36 Torr at 900°C.

The objective of this work is to return to the discussion of this scheme applying a new version of the thermal dissociation mechanism, which is based on the 'dissociative evaporation of the reactant with simultaneous condensation of the low-volatile product'. This approach has been employed earlier to explain the mechanism and kinetics of thermal decomposition of nitrates [16–18], azides [19], carbonates [20], $Li_2SO_4{\cdot}H_2O$ [21], $Mg(OH)_2$ [22], Ag_2O [23], HgO [24] and of a number of other inorganic compounds [25–27].

2. Theoretical

The method to be employed below consists of comparing kinetic parameters derived from experimental data with their theoretical values. The calculations are based on the classical evaporation model of Hertz–Langmuir, extended to the cases of dissociative evaporation of compounds. The scheme of theoretical calculation of the main kinetic parameters (the flux of the gaseous product J, the rate constant k, the product partial pressure P and the parameters of the Arrhenius equation, E_a and A) has been described in a number of previous publications [16–25]. Therefore, we are going to present below only some final relations necessary for the calculations in this work.

In the case of a binary compound S decomposed in vacuo into gaseous products A and B

$$S(s) = aA(g) + bB(g) \quad (9)$$

the flux of product A can be expressed through the equivalent partial pressure P_A (in atm) of this product corresponding to the hypothetical equilibrium of

reaction (9) in the form

$$J_A = \frac{\gamma M P_A}{(2\pi M_A RT)^{1/2}} \quad (10)$$

where M and M_A are the molar masses of the reactant and product A, γ the coefficient of conversion from atmospheres to Pascals, and R the gas constant.

A theoretical value of the partial pressure of product A can be calculated from the equilibrium constant K_p for reaction (9). In the absence of an excess of reaction products in the reactor atmosphere, the situation corresponding to the *equimolar* evaporation mode, the partial pressure P_A can be expressed [26] as

$$P_A^e = a\left(\frac{K_p}{F}\right)^{1/v}\left(\frac{M_A}{M_B}\right)^{b/2v} = \frac{a}{F^{1/v}}\left(\frac{M_A}{M_B}\right)^{b/2v}\exp\left(\frac{\Delta_r S_T^0}{vR}\right)\exp\left(-\frac{\Delta_r H_T^0}{vRT}\right) \quad (11)$$

where

$$F \equiv a^a \times b^b \quad (12)$$

$$v = a + b \quad (13)$$

and

$$K_p = P_A^a \cdot P_B^b \quad (14)$$

Here, $\Delta_r H_T^0$ and $\Delta_r S_T^0$ are, respectively, the changes of the enthalpy and entropy in process (9).

If the partial pressure P'_B of one of the gaseous components greatly exceeds the equivalent pressure P_B of the same component released in the decomposition and if, in addition to that, the magnitude of P'_B remains constant in the process of decomposition, we call such evaporation mode *isobaric*. In this case,

$$P_A^i = \frac{K_p^{1/a}}{(P'_B)^{b/a}} = \frac{1}{(P'_B)^{b/a}}\exp\left(\frac{\Delta_r S_T^0}{aR}\right)\exp\left(-\frac{\Delta_r H_T^0}{aRT}\right) \quad (15)$$

As can be seen from Eqs. (11) and (15), the calculated activation energies for reaction (9) should be different for the equimolar and isobaric modes of decomposition, i.e.

$$E_a^e = \frac{\Delta_r H_T^0}{\gamma} \quad (16)$$

for the equimolar mode and

$$E_a^i = \frac{\Delta_r H_T^0}{a} \quad (17)$$

for the isobaric one.

In order to take into account the partial transfer of the energy released in the condensation of low-volatile A product to the reactant, we introduced, as before [21–24], into calculations of the enthalpy of decomposition reaction (9) an additional term $\tau a \Delta_c H_T^0(A)$, where the coefficient τ corresponds to the fraction of the condensation energy transferred to the reactant. Thus, we can write

$$\Delta_r H_T^0 = a\Delta H_T^0(A) + b\Delta H_T^0(B) - \Delta H_T^0(S) + \tau a \Delta_c H_T^0(A) \quad (18)$$

Table 1 lists the values of the thermodynamic functions [28–30] for the reactions being discussed without considering the condensation energy transfer. The most plausible of all conceivable mechanisms of the energy transfer appears to be the thermal accommodation [31] or, in other words, direct transfer of the energy at the reaction interface in collisions of the low-volatile molecules with the reactant and product surface. For equal temperatures of the solid phases, one may expect equipartition of energy between the two phases, i.e. τ=0.5.

3. Results and discussion

3.1. Autocatalysis

The characteristic property of carbothermal reduction of Fe, Co, Ni and Cu oxides is their autocatalytic development. It means that the rate of isothermal reduction accelerates as the reduction progresses, and passes through a maximum. Representative examples of variation of the rate of reduction with degree of reduction in vacuum for Fe and Cu oxides are reproduced from publications by Chufarov and co-workers [32,33] in Figs. 1 and 2.

Under these conditions, the reduction curves, $\alpha = f(t)$, have a sigmoid shape typical for many decomposition reactions. As an illustration, the family of reduction curves for NiO in a flow of argon taken

Table 1
Thermodynamic functions [28–30]

Reaction	$\Delta_r H_T^0$ (kJ mol^{-1})			$\Delta_r S_T^0$ (J mol^{-1} K^{-1})		
	1000 K	1300 K	1600 K	1000 K	1300 K	1600 K
Fe (s)=Fe (g)	409.5	402.1	398.0	143.4	136.7	131.0
FeO (s)=Fe (g)+$\frac{1}{2}O_2$	675.7	669.4	662.6	205.2	199.7	195.0
FeO (s)=Fe (s)+ $\frac{1}{2}O_2$	266.1	267.4	264.6	61.8	63.0	64.1
Co (s)=Co (g)	424.5	419.9	414.7	143.8	139.7	136.1
CoO (s)=Co (g)+ $\frac{1}{2}O_2$	662.9	659.1	654.0	213.5	210.0	206.8
CoO (s)=Co (s)+ $\frac{1}{2}O_2$	238.4	239.2	239.3	69.7	70.3	70.6
Ni (s)=Ni (g)	424.2	421.3	417.7	144.7	142.0	139.6
NiO (s)=Ni (g)+ $\frac{1}{2}O_2$	663.5	659.5	653.6	230.4	226.8	223.4
NiO (s)=Ni (s)+ $\frac{1}{2}O_2$	239.3	238.2	236.8	85.7	84.8	83.8
Cu (s)=Cu (g)	332.8	330.8	315.8[a]	126.2	124.0	113.1[a]
Cu_2O (s)=2Cu (g)+ $\frac{1}{2}O_2$	838.8	830.5	822.8[a]	319.2	313.5	308.3[a]
Cu_2O (s)=2Cu (s/l)+ $\frac{1}{2}O_2$	172.8	168.8	187.8[a]	66.0	65.5	82.2[a]

[a] At 1500 K.

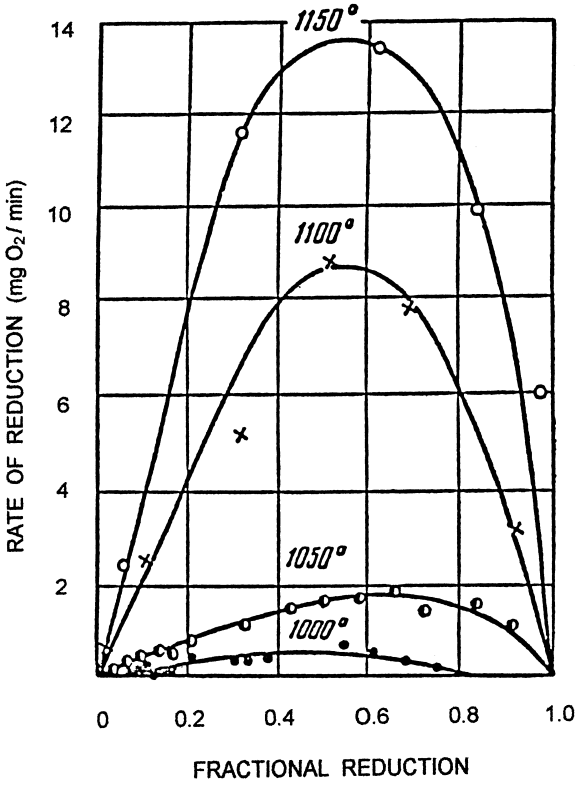

Fig. 1. Reduction of FeO by carbon in vacuum at different temperatures (in °C). Reproduced from [32] by permission of the Journal Editor.

from the paper by Ashin et al. [34] are presented in Fig. 3. A very long induction period in this case is worth noting.

The origin of these induction and acceleration periods has been interpreted recently in the framework of the mechanism of congruent dissociative evaporation with simultaneous condensation of the low-volatility product at the reactant/product interface [23,27]. The essence of this approach consists in the partial transfer of the condensation energy to the reactant (oxide) and, as a result, increasing of its decomposition rate. In the initial decomposition stage, in the absence of any nuclei on the reactant surface, which provide condensation of the vapour of the low-volatile product at the interface zone and energy transfer to the reactant, the decomposition proceeds much slower. The time taken to form the first nuclei on the surface of the reactant corresponds to the induction period. In the framework of this approach, the mechanism of nucleation through condensation of supersaturated vapour of the low-volatility product (metal) becomes obvious as well [31].

The presence of defects or foreign impurities on the surface turns out to be equivalent to the appearance of nuclei of a new phase. Because of this, the induction and acceleratory periods, in which the product film covers the whole surface of reactant and the reaction reaches steady state, become shorter or disappear

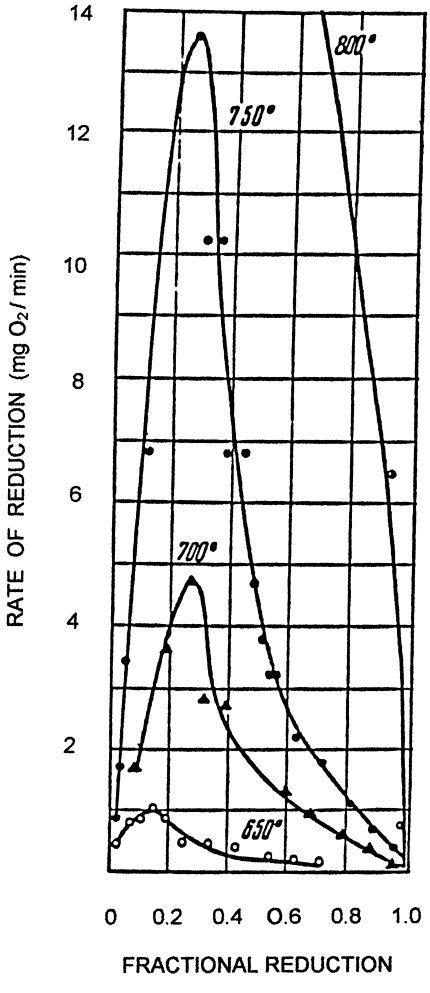

Fig. 2. Reduction of Cu_2O by carbon in vacuum at different temperatures (in °C). Reproduced from [33] by permission of the Journal Editor.

completely. It is well-supported by experiments performed by Ashin et al. [34]. As can be seen from the comparison of the reduction curves for NiO in argon in the absence (Fig. 3) and in the presence of addition of metallic nickel (Fig. 4), the total reduction time in the last case is about 10 times less (taking into account the difference in the lowest temperature of experiments: 720 and 700°C, respectively). As would be expected, the induction period in the presence of a large addition of nickel (50%) practically disappeared, but the steady state rate of decomposition was the same irrespective of the amount of metal (12.5 or 50%).

3.2. Initial temperatures

As a criteria for the theoretical estimation of initial temperatures of reduction, we will use two practically important parameters: the average initial radius of oxide particles, r_0 and the total time of decomposition (reduction), t_0. Upon integration of equation

$$J = -\left(\frac{\mathrm{d}m}{\mathrm{d}t}\right)(4\pi r^2)^{-1} \tag{19}$$

and taking into account Eq. (10) and the obvious relationship: $m=(4/3)\pi r^3\rho$, where m, r and ρ are the mass, radius and density of reactant spherical particle(s), respectively, we obtain a simple expression

$$P_\mathrm{B} = \left[\frac{\rho(2\pi M_\mathrm{B}RT)^{1/2}}{\gamma M}\right]\left(\frac{r_0}{t_0}\right) \tag{20}$$

Substituting the average for Fe, Co, Ni and Cu values of parameters: $\rho=6500$ kg m^{-3}; $M_\mathrm{B}=0.032$ kg mol^{-1}; $M=0.075$ kg mol^{-1}, we obtain for the partial pressure of oxygen

$$P(\mathrm{O_2}) \cong 35\left(\frac{r_0}{t_0}\right) \tag{20}$$

Here, $P(O_2)$ is expressed in atm, r_0 in m and t_0 in s. Assuming $r_0=10$ μ$=1\times10^{-5}$ m and $t_0=1$ h$=3600$ s, we have $P(O_2)\cong1\times10^{-7}$ atm.

Table 2 lists the initial temperatures for the thermal decomposition of oxides calculated at $P(O_2)=1\times10^{-7}$ atm and $\tau=0.5$, using Eqs. (11) and (18) and the thermodynamic functions from Table 1. The experimental values [32–42] were obtained by different techniques and under very different experimental conditions: some in vacuum and some in a flow of argon at atmospheric pressure. Nevertheless, as can be seen from the comparison of these data, the discrepancy between calculated and experimental values does not exceed 100 K for Fe, Co and Cu. In the case of Ni, about a 200 K systematic discrepancy is observed. It can be partly connected with a smaller particle size in NiO powders used in experiments. Indeed, as it was noted by Tumarev et al. [43], the size of NiO particles in powders prepared via the decomposition of $Ni(NO_3)_2$, is typically one-two orders of magnitude smaller than that for the standard chemicals. Pavlyuchenko and Shelkantseva [38] who observed the initial reduction of NiO at 873 K, used

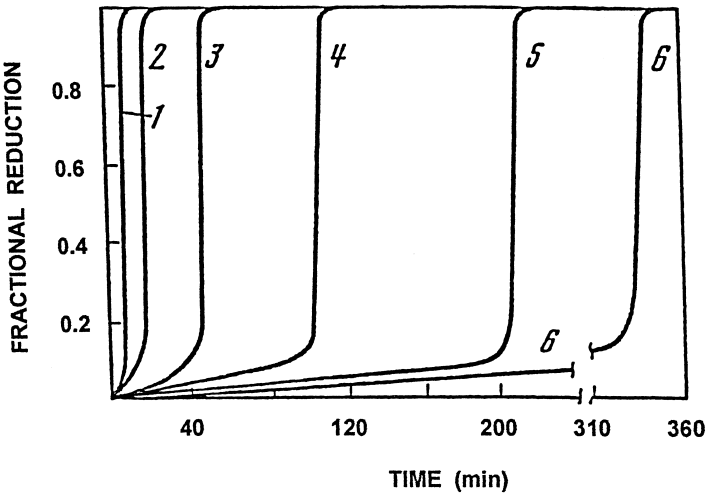

Fig. 3. Reduction of NiO by carbon in a flow of argon (67 ml min^{-1}) at different temperatures (°C): (1) 920; (2) 880; (3) 840; (4) 800; (5) 760 and (6) 720. Reproduced from [34].

NiO samples prepared from $Ni(NO_3)_2$. Therefore, as a whole, the agreement between the theoretical and experimental values of initial decomposition temperatures may be considered as more than satisfactory.

3.3. Activation energies

Figs. 5–8 illustrate the Arrhenius plots for the carbothermal reduction of Fe, Ni and Cu oxides constructed by the author on the basis of experimental results presented in different works in graphical or tabular form. The standard linear regression program was used for computing the activation energies and standard deviations. These data together with the theoretical results calculated from formulas (16) and (17) are listed in Table 3. The value of τ-parameter in calculating $\Delta_r H_T^0$ was taken to be 0.5, as before.

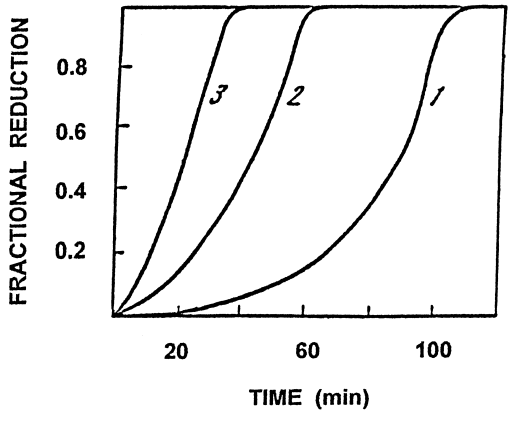

Fig. 4. Reduction of NiO by carbon in a flow of argon at 700°C in the presence of different additions of Ni (%): (1) 12.5; (2) 25 and (3) 50. Reproduced from [34].

It should be noted that the different parameters were plotted along the ordinate axes in different figures. In Fig. 5, the mass of oxygen loss (J) by 1 g of oxide in 1 min (see Figs. 1 and 2) was plotted. In Figs. 6 and 7, the k_1-coefficient in the Prout–Tompkins equation [44] and the rate constant k_2 for the first-order kinetics were plotted, respectively. In Fig. 8, the k_3-coefficient inverse of time interval from the start of oxide heat-treating to the moment of its 20% reduction (see Fig. 3) was plotted. However, in spite of this difference, these plots can be compared in their position along a temperature scale.

It is interesting, in particular, to compare the Arrhenius plots for the reduction of FeO reproduced in Figs. 5–7. As can be seen from these figures and the results presented in Table 3, there are two sets of activation energies (slopes of the Arrhenius plots) which are distinguished by a factor 1.5 on the average. This fact is in excellent agreement with the theoretical expectation of the two different modes (isobaric and equimolar) for the dissociative evaporation scheme while there is no reasonable explanation in the framework of a reduction mechanism. Recall that the

Table 2
Initial temperatures for thermal decomposition of oxides

Oxide	T_{calc} (K)[a]	T_{expt} (K) [Reference]	
		Vacuum	1 atm of Ar
FeO	1285	1270 [32], 1260 [36]	1250 [39], 1173 [40], 1225 [41], 1180 [42]
CoO	1195	1100 [35]	
NiO	1045	923 [35], 873 [38]	973 [34], 923 [40]
Cu_2O	850	900 [33], 900 [37]	800 [40]

[a] At $P(O_2)=10^{-7}$ atm and $\tau=0.5$.

conception of isobaric and equimolar modes was introduced by L'vov and Fernandes [45] in 1984 as a result of investigations into the thermal dissociation kinetics of metal oxides by electrothermal atomic absorption spectrometry. Later on, this conception has been used [21,26,27] for the interpretation of the same peculiarities observed in other decomposition reactions, in particular, in the process of decomposition (dehydration) of some hydrated salts [46,47].

It must be emphasised that, as expected, the isobaric mode in the case of FeO decomposition has been observed only under conditions of argon flow when the partial pressure of residual oxygen in Ar is in excess of the equivalent pressure of O_2 (1×10^{-7} atm) at the initial temperature. Such a situation is unlikely in high vacuum. The difference in the decomposition modes observed by Szedrei and van Berge [41] and Rao [42] at high temperatures (>1230 K) is, probably, due to the different content of O_2 in argon. It is supported by a remark in [42] that a purified argon gas was used in this work. In this case (Fig. 7), two regions are observed in the Arrhenius plot: isobaric and equimolar, at lower and higher temperatures, respectively.

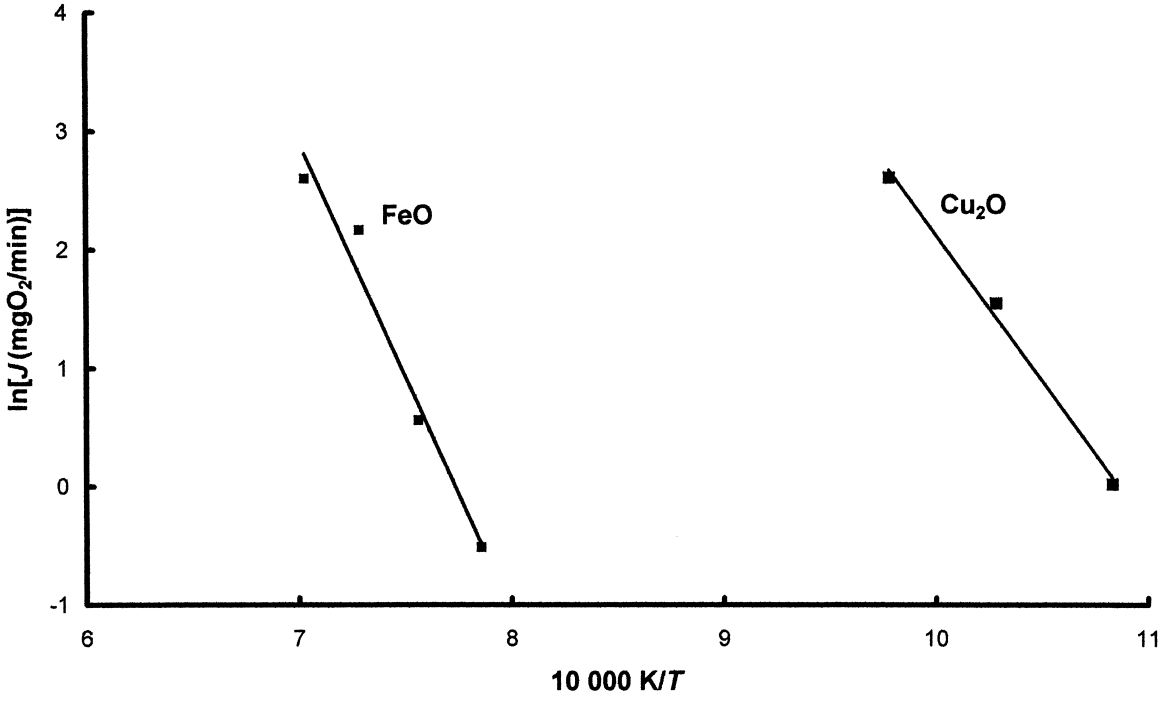

Fig. 5. Arrhenius plots for the carbothermal reduction of FeO and Cu_2O constructed from data extracted from [32,33].

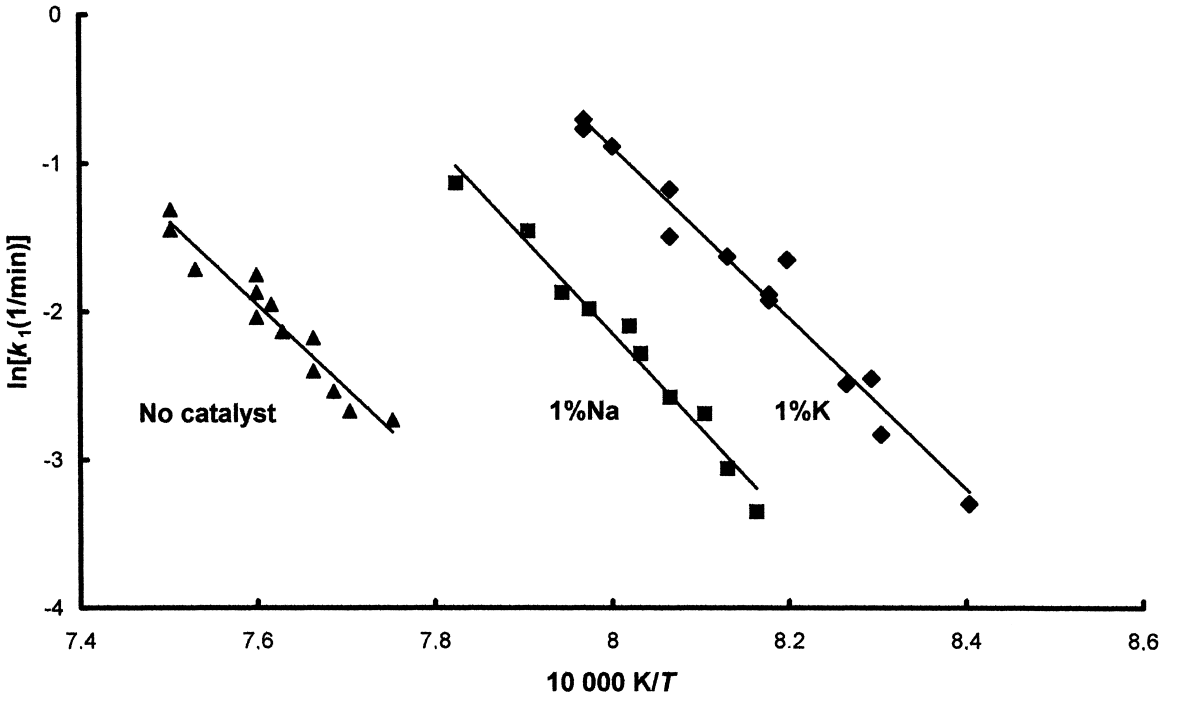

Fig. 6. Arrhenius plots for the carbothermal reduction of FeO constructed from data extracted from [41].

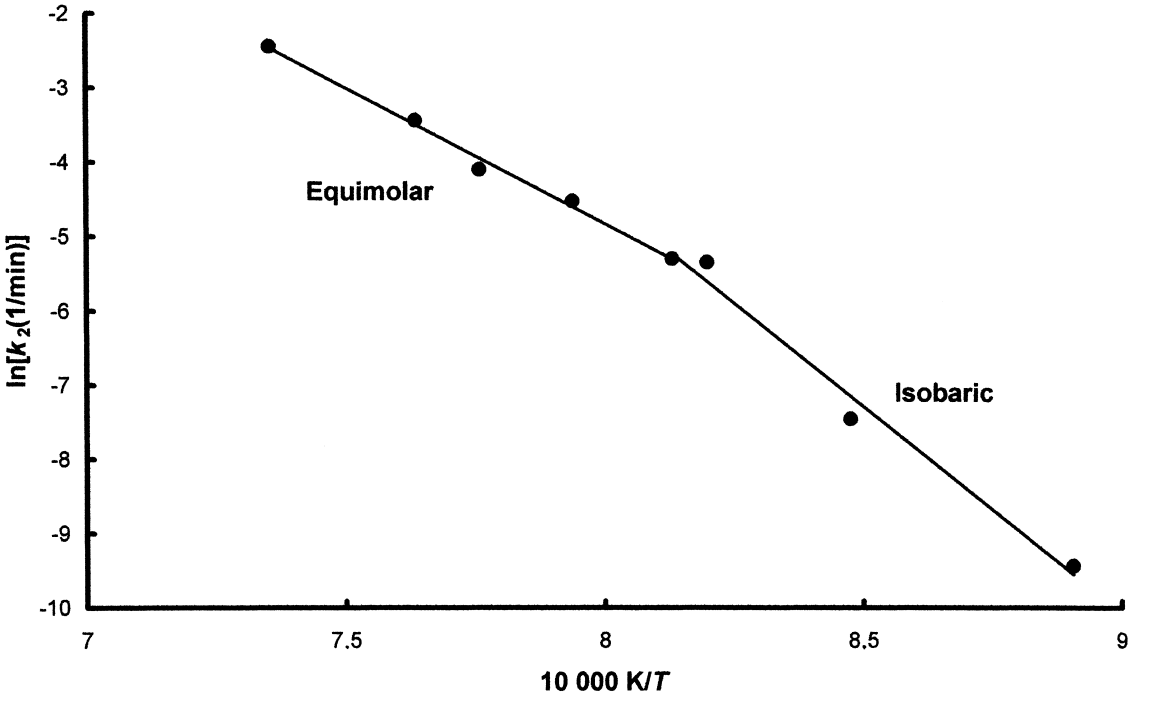

Fig. 7. An Arrhenius plot for the carbothermal reduction of FeO constructed from data extracted from [42].

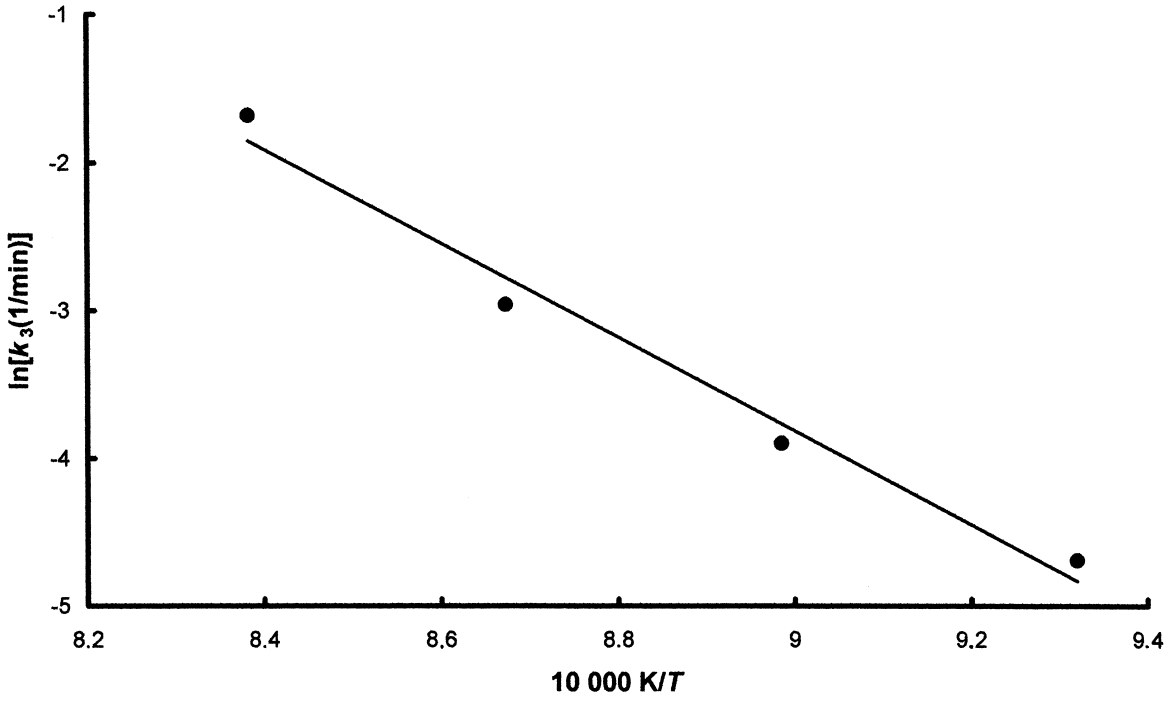

Fig. 8. An Arrhenius plot for the carbothermal reduction of NiO constructed from data extracted from [34].

One further peculiarity of the plots presented in Fig. 6 is the strong effect of Na_2CO_3 and K_2CO_3 additions on the rate of carbothermal reduction. We attribute this to a decreasing partial pressure of O_2 in the argon flow due to the activation of reducing properties of graphite in the presence of alkali metals. In its turn, this activation is, probably, a result of formation and subsequent decomposition (at a high temperature) of lamellar compounds of Na and K with carbon with a consequent structural deformation of graphite particles [48]. The activation effect of alkalis on graphite was confirmed by the experiments described in [36]. The shift of the plot in the presence of 1% K_2CO_3 to the lower temperature (Fig. 6) corresponds to a 28-fold increase of the rate constant or about three-orders of magnitude (28^2) decrease of partial pressure of O_2. This is possible if the initial concentration of O_2 in argon in experiments [41] was $\geq$0.1%.

3.4. Oxide decomposition in effusion (Knudsen) cells

One of the consequence resulting from the proposed mechanism of the carbothermal reduction of oxides through the dissociative evaporation of oxide with simultaneous condensation of metal is a possibility

Table 3
Activation energies for thermal decomposition of oxides

Oxide	E_a (kJ mol^{-1})	
	Calculated	Experimental
FeO	312 (Equimolar mode)	331±43 [32], 305±25 [42]
	468 (Isobaric mode)	465±32 [41], 534±31 [41], 479±27 [41], 463±40 [42]
NiO	300 (Equimolar mode)	264±27 [34]
Cu_2O	202 (Equimolar mode)	205±17 [33]

Table 4
Equilibrium pressures and activation energies for the gaseous (imaginary) dissociation of oxides and evaporation of metals

Oxide	T (K)	P_M (atm)		E_a (kJ mol^{-1})	
		Dissociation	Evaporation	Dissociation	Evaporation
FeO	1700	2.1×10^{-7}	4.1×10^{-6}	442	398
CoO	1700	8.0×10^{-7}	2.3×10^{-6}	436	415
NiO	1700	3.1×10^{-6}	3.0×10^{-6}	436	417
Cu_2O	1500	1.3×10^{-5}	8.1×10^{-6}	329	316
	1300	2.1×10^{-7}	1.5×10^{-7}	332	331

of a realisation of this process in the absence of carbon. Actually, the role of carbon in this process is to react with the oxygen liberated from the decomposition of the oxide, thus, maintaining a low partial pressure of oxygen in the system. It is impossible to extract O_2 from this volume under atmospheric pressure of foreign (inert) gas because of the diffusion limitations. However, in a high vacuum, this extraction should be efficient enough. This suggests that the dissociative evaporation of oxide with simultaneous condensation of metal can be observed in high vacuum in the absence of carbon.

With this purpose in mind, we carefully analysed the results of investigation of dissociation of FeO, CoO, NiO and Cu_2O in an effusion (Knudsen) cell [49]. It was found that these oxides dissociate with the formation of solid metals inside the cell. It was proved, in particular, by direct observation of Co and Ni metals on the interior surfaces of the Knudsen cells [50–52]. This result is in contradiction with that expected from thermodynamic equilibrium

$$MO(s) = M(g) + \tfrac{1}{2}O_2 \quad (22)$$

Indeed, as can be seen from the results presented in Table 4, the calculated equilibrium partial pressures of Ni and Cu for the gaseous dissociation of their oxides are comparable with the equilibrium pressures of metal vapour over solid metals, but for Fe and Co, they are much smaller. At lower temperatures, this difference is even higher. This is evident from the comparison of the activation energies for these two processes (Table 4). Therefore, if the mechanism of dissociation obeyed the equilibrium shown by Eq. (22), the formation of metal in the condensed phase (solid or liquid) is improbable (for Ni and Cu) or impossible (for Fe and Co).

The only explanation of the metal appearance in Knudsen cells is that the real mechanism of dissociation of these oxides consists in their dissociative evaporation with the simultaneous condensation of metal vapour at the oxide/metal interface and partial transfer of the condensation energy to the oxide. This process (at τ=0.5) proceeds at much lower temperatures than the simple gaseous dissociation of oxide without taking into account the energy transfer (τ=0). If this is the case, it can be expected in addition that the partial pressure of O_2 effused from the Knudsen cell is higher than the equilibrium pressure over MO(s)–M(s) system. As can be seen from the data presented in Table 5, the experimental partial pressures of oxygen in almost all known publications [52–56] are an order of magnitude higher than the equilibrium pressures for the condensate dissociation of oxides

$$MO(s) = M(s) + \tfrac{1}{2}O_2 \quad (23)$$

Therefore, both these facts (the appearance of metals in the condensed phase and higher than equilibrium partial pressure of oxygen) can be considered as additional arguments in support of the mechanism proposed.

Table 5
Partial pressures of oxygen calculated for the condensate (imaginary) dissociation of oxides (23) and experimental data measured by effusion mass spectrometry

Oxide	T (K)	P (atm)	
		Calculated	Experimental
CoO	1600	6×10^{-9}	5×10^{-8} [52], 1×10^{-7} [53]
NiO	1500	2×10^{-8}	4×10^{-8} [54], 8×10^{-8} [55]
Cu_2O	1300	2×10^{-7}	2×10^{-6} [56], 1.3×10^{-6} [54]

4. Conclusions

The main conclusion that follows from the above analysis is that the process of carbothermal reduction of iron, cobalt, nickel and copper oxides is actually the decomposition process typical for many other types of solid state decomposition reactions. It can be described in the framework of the mechanism of dissociative evaporation of oxide with the simultaneous condensation of metal at the oxide/metal interface. Some important features of carbothermal reduction process, such as initial temperatures and activation energies, were quantitatively interpreted on this basis. The origin of the induction and acceleration periods in the development of reduction has been explained. The function of carbon in this process is to react with the oxygen liberated from the decomposition of the oxide, thus maintaining a low partial pressure of oxygen in the system. In another words, carbon fulfils the role of buffer in this process. This conclusion is supported by an appearance of metals in the condensed phase and a higher than equilibrium partial pressure of oxygen in the high-vacuum experiments with Knudsen cells.

One might expect that a similar process of 'carbothermal reduction' occurs for oxides of some other metals like metals of platinum group, Ag and Au. The oxides of these elements are not stable and the volatility of these metals at decomposition temperatures below 1000 K is very low. At the same time, this mechanism does not work, if the metal remains in the gaseous phase at the temperature of oxide reduction. This is true for the oxides of elements like Al, Cr, Mg, Mn, Sn, Zn, etc. Their carbothermal reduction occurs most probably via the gaseous carbide mechanism [10,11].

References

[1] M. Beckert, Eisen. Tatsachen und Legenden, VEB Deutscher Verlag, Leipzig, 1981.
[2] Yu. S. Yusfin, V.V. Dan'shin, N.F., Pashkov, V.A. Pitatelev, Theory of Metallization of Iron-Contained Raw Materials, Metallurgiya, Moscow, 1982 (in Russian).
[3] L. Gruner, Traite de Metallurgie Generale, Paris, 1875.
[4] A.A. Baikov, Metallurgy 3 (1926) 5–24.
[5] M.A. Pavlov, Metallurgy of Cast Iron, Kubuch, Leningrad, 1935 (in Russian).
[6] G.I. Chufarov, Dissertation, Institute of Chem. Physics, Kubuch, Leningrad, 1937 (in Russian).
[7] O.A. Esin, P.V. Gel'd, Uspechi Khim. 18 (1949) 658–681.
[8] B.V. L'vov, Dokl. Akad. Nauk SSSR 271 (1983) 119–121.
[9] B.V. L'vov, Spectrochim. Acta, Part B 44 (1989) 1257–1271.
[10] B.V. L'vov, L.K. Polzik, N.P. Romanova, A.I. Yuzefovskii, J. Anal. At. Spectrom. 5 (1990) 163–169.
[11] B.V. L'vov, A.A. Vasilevich, A.O. Dyakov, W.H. Lam, R.E. Sturgeon, J. Anal. At. Spectrom. 14 (1999) 1019–1024.
[12] S.V. Digonskii, New Methods of Metal Production from their Oxidised Compounds, Nauka, St. Petersburg, 1998 (in Russian).
[13] G. Tammann, A. Sworykin, Z. Anorg. Allg. Chem. 170 (1928) 62–70.
[14] A.A. Baikov, A.S. Tumarev, Izv. Akad. Nauk SSSR 1 (1937) 25–45.
[15] M.M. Kurchatov, Zh. Fiz. Khim. 32 (1958) 2586–2593.
[16] B.V. L'vov, Mikrochim. Acta (Wien) II (1991) 299–308.
[17] B.V. L'vov, A.V. Novichikhin, Spectrochim. Acta, Part B 50 (1995) 1427–1448.
[18] B.V. L'vov, A.V. Novichikhin, Spectrochim. Acta, Part B 50 (1995) 1459–1468.
[19] B.V. L'vov, Thermochim. Acta 291 (1997) 179–185.
[20] B.V. L'vov, Thermochim. Acta 303 (1997) 161–170.
[21] B.V. L'vov, Thermochim. Acta 315 (1998) 145–157.
[22] B.V. L'vov, A.V. Novichikhin, A.O. Dyakov, Thermochim. Acta 315 (1998) 135–143.
[23] B.V. L'vov, Thermochim. Acta 333 (1999) 13–19.
[24] B.V. L'vov, Thermochim. Acta 333 (1999) 21–26.
[25] B.V. L'vov, A.V. Novichikhin, Thermochim. Acta 290 (1997) 239–251.
[26] B.V. L'vov, Spectrochim. Acta, Part B 52 (1997) 1–23.
[27] B.V. L'vov, Spectrochim. Acta, Part B 53 (1998) 809–820.
[28] V.A. Kireev, Methods of Practical Calculations in Thermodynamics of Chemical Reactions, Khimiya, Moscow, 1975 (in Russian).
[29] V.A. Ryabin, M.A. Ostroumov, T.F. Svit, Thermodynamic Characteristics of Substances, Handbook, Khimiya, Leningrad, 1977 (in Russian).
[30] L.V. Gurvich, I.V. Veits, V.A. Medvedev, et al., Thermodynamic Properties of Individual Substances, Nauka, Moscow, 1978–1982 (in Russian).
[31] J.P. Hirth, G.M. Pound, Condensation and Evaporation, Pergamon Press, Oxford, 1963.
[32] V.I. Arkharov, V.N. Bogoslovskii, M.G. Zhuravleva, G.I. Chufarov, Zh. Fiz. Khim. 29 (1955) 272–279.
[33] E.P. Tatievskaya, G.I. Chufarov, N.M. Stafeeva, Zh. Fiz. Khim. 28 (1954) 843–850.
[34] A.K. Ashin, S.T. Rostovtsev, O.L. Kostelov, in: Reduction Processes in the Production of Ferroalloys, Nauka, Moscow, 1977, pp. 174–178 (in Russian).
[35] M.G. Zhuravleva, G.I. Chufarov, AN SSSR (Ural Filial), Trudy Instituta Metallurgii 3 (1959) 63–66.
[36] M.G. Zhuravleva, G.I. Chufarov, L.G. Khromykh, Dokl. AN SSSR 135 (1960) 385–388.
[37] M.M. Pavlyuchenko, N.A. Shelkantseva, in: Heterogeneous Chemical Reactions, Vysshaya Shkola, Minsk, 1961, pp. 212–224 (in Russian).

[38] M.M. Pavlyuchenko, N.A. Shelkantseva, in: Heterogeneous Chemical Reactions, Nauka i Tekhnika, Minsk, 1965, pp. 150–161 (in Russian).
[39] S.T. Rostovtsev, V.K. Simonov, A.K. Ashin, O.L. Kostelov, in: Mechanism and Kinetics of Reduction of Metals, Nauka, Moscow, 1970, pp. 24–31 (in Russian).
[40] M.A. Vishkarova, V.V. Levina, D.I. Ryzhonkov, G.R. Umarov, Izv. Vuzov. Chem. Metallurgiya 9 (1996) 1–3.
[41] T. Szendrei, P.C. van Berge, S. Afr. J. Chem. 31 (1978) 51–58.
[42] Y.K. Rao, Metall. Trans. 2 (1971) 1439–1447.
[43] A.S. Tumarev, V.A. Pushkarev, L.N. Pushkareva, in: Reduction Processes in the Production of Ferroalloys, Nauka, Moscow, 1977, pp. 178–182 (in Russian).
[44] E.G. Prout, F.C. Tompkins, Trans. Faraday Soc. 40 (1944) 488–498.
[45] B.V. L'vov, G.H.A. Fernandes, Zh. Anal. Khim. 39 (1984) 221–231.
[46] D. Dollimore, T.A. Evans, Y.F. Lee, F.W. Wilburn, Thermochim. Acta 198 (1992) 249–257.
[47] M.M. Pavlyuchenko, V.V. Samuskevich, E.A. Prodan, Izv. AN BSSR, Ser. Khim. Nauk 6 (1970) 11–15.
[48] A.R. Ubbelohde, F.A. Lewis, Graphite and its Crystal Compounds, Clarendon Press, Oxford, 1960.
[49] E.K. Kazenas, D.M. Chizhikov, Pressure and Composition of Vapour under Oxides of Chemical Elements, Nauka, Moscow, 1976 (in Russian).
[50] L. Brewer, D. Mastick, J. Chem. Phys. 19 (1951) 834–843.
[51] R.T. Grimley, R.P. Burns, M.G. Inghram, J. Chem. Phys. 35 (1961) 551–554.
[52] R.T. Grimley, R.P. Burns, M.G. lnghram, J. Chem. Phys. 45 (1966) 4158–4162.
[53] D.M. Chizhikov, Yu.V. Tsvetkov, E.K. Kazenas, V.K. Tagirov, Zh. Neorg. Khim. 17 (1972) 891–894.
[54] K. Kodera, I. Kusunoki, S. Shimizu, Bull. Chem. Soc. Jpn. 41 (1968) 1039.
[55] E.K. Kazenas, D.M. Chizhikov, Yu.V. Tsvetkov, in: Investigation of the Processes in Metallurgy of Non-Ferrous and Rare Metals, Nauka, Moscow, 1969, pp. 28–29 (in Russian).
[56] E.K. Kazenas, D.M. Chizhikov, Yu.V. Tsvetkov, Izv. AN SSSR, Metally 2 (1969) 60–62.